

Thermal stability of semi-insulating InP epilayers: The roles of dicarbon and carbon-hydrogen centers

R. C. Newman and B. R. Davidson

Centre for Electronic Materials and Devices, The Blackett Laboratory, Imperial College of Science, Technology and Medicine, London SW7 2BZ, United Kingdom

J. Wagner

Fraunhofer-Institut für Angewandte Festkörperphysik, Tullastrasse 72, D-71908 Freiburg, Federal Republic of Germany

M. J. L. Sangster* and R. S. Leigh

J. J. Thomson Physical Laboratory, University of Reading, P.O. Box 220, Whiteknights, Reading RG6 6AF, United Kingdom

(Received 1 November 2000; published 20 April 2001)

Infrared- (IR) absorption measurements of localized vibrational modes (LVM's) show the presence of H-C_p pairs and isolated C_p acceptors in semi-insulating epitaxial layers of InP. Rapid transient anneals of two sets of such samples at temperatures of up to 800 °C lead to the complete loss of the H-C_p pairs and large decreases of [C_p], from initial values of 5.8×10^{18} and $2.5 \times 10^{18} \text{ cm}^{-3}$. The layers remain semi-insulating up to 700 °C and, even after annealing at 800 °C, they show only low *n*-type conductivities ($n \sim 10^{16} \text{ cm}^{-3}$), implying the continued presence of a sufficient concentration of donor centers to effect near compensation. Raman scattering measurements reveal LVM's (IR inactive), close to 1800 cm^{-1} and broadbands, due to amorphous carbon, that show increased strengths after annealing. The LVM's are attributed to deep donor dicarbon split-interstitial centers occupying phosphorus lattice sites, analogous to corresponding centers observed in annealed highly carbon-doped *p*-type GaAs and AlAs that have been investigated by local-density-functional calculations. No evidence is found for the presence of shallow donors, namely V_{In}H₄ complexes, C_{In} donors or P_{In} antisite defects. Changes in the unusual electric-field broadening of the C_p LVM, revealed by IR measurements, are related to the reductions in the concentration of C_p defects resulting from the anneals. These calculations give further insight about the compensating defects and may imply reductions in strain after the higher-temperature anneals.

DOI: 10.1103/PhysRevB.63.205307

PACS number(s): 81.15.Gh, 81.05.Ea, 66.30.Jt, 63.20.Pw

I. INTRODUCTION

Semi-insulating InP layers can be grown by metal-organic vapor-phase epitaxy (MOVPE) in the temperature range 460–500 °C using PH₃ and trimethyl-indium precursors, provided the layers are doped with carbon derived from CCl₄ entrained in hydrogen gas.^{1,2} Secondary ion mass spectrometry (SIMS) measurements show only small concentrations of incorporated chlorine and oxygen but the layers contain both carbon and hydrogen at concentrations as high as 10^{18} – 10^{20} cm^{-3} . An explanation of the high resistivity was unclear. Early work had implied that carbon atoms might occupy either group-III or -V lattice sites,^{3–5} but later analyses of infrared (IR) localized vibrational mode (LVM) absorption measurements^{6,7} showed that the observed carbon atoms were *acceptors* occupying phosphorus lattice sites, as isolated ¹²C_p (and ¹³C_p, 1.1% abundant), and as H-¹²C_p (and H-¹³C_p) pairs, found also in GaAs.⁸ The identity of the incorporated donors at the high concentration required to effect compensation has remained unknown but it was speculated that undetected V_{In}H₄,^{9,10} C_{In} and P_{In} double donor antisite defects¹¹ might be present. Any excess of these shallow centers over the isolated carbon acceptor concentration would, however, make the samples strongly *n* type, contrary to the measurements.

In this paper we present LVM IR absorption and LVM Raman scattering measurements for such samples following

anneals at temperatures in the range 500–800 °C. IR measurements show small initial increases in the strength of the absorption from C_p and decreases of [H-C_p] pairs following anneals at 500 °C, the same as the growth temperature, but anneals at higher temperatures lead to progressive reductions of the concentrations of both centers. These measurements allow us to demonstrate that the strengths of the three IR-active modes, tentatively attributed to H-¹²C_p pairs,^{6,7} are indeed correlated and Raman scattering measurements provide evidence that one of the lines is a doubly degenerate *E* mode, as expected. The Raman measurements also reveal amorphous carbon and, more importantly, dicarbon split-interstitial pairs (both IR inactive) at essentially the same frequencies as those found in annealed *p*-type GaAs:C_{As} (Ref. 12) and AlAs:C_{As}.¹³ Theoretical analyses^{13,14} of such C-C centers have shown that they are deep donors. The compensating donors in InP are therefore assigned to similar C-C centers.

The ¹²C_p LVM at 546.9 cm^{-1} (10 K) lies in the gap from 517.5 to 612.4 cm^{-1} of the density of two-phonon states¹⁵ of the InP lattice and was expected to have a small full width at half maximum Δ , since the decay of the excitation requires the formation of at least three phonons. For comparison we find that the LVM of isoelectronic ¹⁰B_{In} at 543.56 cm^{-1} in InP has a Δ of only 0.07 cm^{-1} for bulk material measured at an instrumental resolution of 0.01 cm^{-1} : this line was reported in much earlier work.¹⁶ However, measurements have

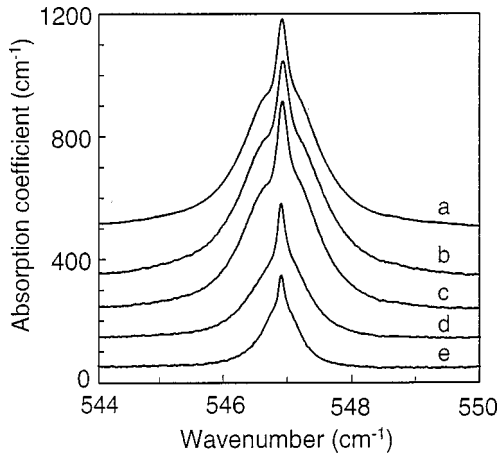


FIG. 1. Broadening of the C_p IR LVM shown on an expanded wave-number scale for sample MR949 after the growth of the layer and following anneals at progressively increasing temperatures when the concentration of isolated carbon acceptors is reduced. The letters *a,b,c,d,e* refer to the as-grown sample and other samples following anneals at 500 °C, 600 °C, 700 °C, and 800 °C.

shown that the $^{12}C_p$ line is always significantly broadened ($\Delta \sim 1 \text{ cm}^{-1}$) with an unusual profile that has a sharp central feature (Figs. 1 and 2). This structure has been attributed to perturbations of the negatively charged $^{12}C_p^-$ acceptors by internal electric fields, having random strengths and directions, that arise from the surrounding *immobile* charges of all other isolated C_p^- acceptors and positively charged compensating donors.¹⁷ After samples are annealed there are reductions of the linewidth of the C_p LVM implying reductions in the magnitude of the internal electric fields due to reductions in $[C_p]$ and the concentration of ionized donors. The observations also imply the absence of free carriers that would otherwise screen the electric field at the locations of the C_p atoms.

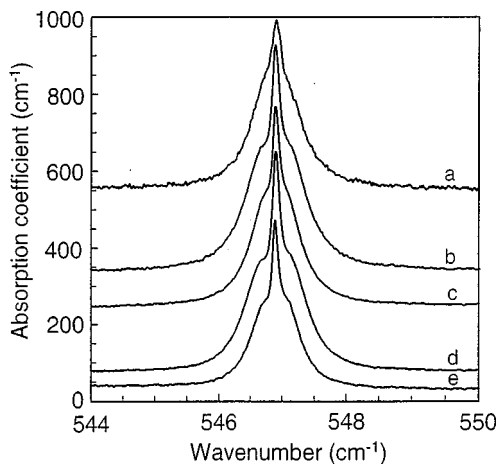


FIG. 2. Broadening of the C_p IR LVM shown on an expanded wave-number scale for sample MR950 after the growth of the layer and following anneals at progressively increasing temperatures when the concentration of isolated carbon acceptors is reduced. The letters *a,b,c,d,e* refer to the as-grown sample and other samples following anneals at 500 °C, 600 °C, 700 °C, and 800 °C.

TABLE I. Concentrations of $[C_p] \times 10^{18} \text{ cm}^{-3}$ (LVM at 546.9 cm^{-1}) and $[H-C_p] \times 10^{18} \text{ cm}^{-3}$ (LVM at 2703 cm^{-1}) for sample MR949 (thickness $8 \times 10^{-4} \text{ cm}$) and MR950 (thickness $10.3 \times 10^{-4} \text{ cm}$), with the assumptions that $f(C_p) = 7 \times 10^{15} \text{ cm}^{-1}$ and $f(H-C_p) = 2 \times 10^{15} \text{ cm}^{-1}$.

Anneal temperature (°C)	MR949 $[C_p]$ 546.9 cm^{-1}	MR949 $[H-C_p]$ 2703 cm^{-1}	MR950 $[C_p]$ 546.9 cm^{-1}	MR950 $[H-C_p]$ 2703 cm^{-1}
As grown	5.8	5.4	2.5	1.4
500	6.6	4.6	3.3	1.3
600	5.3	2.6	2.6	1.0
700	2.5	0.7	3.0	0.1
800	1.3	0.0	1.9	0.0

II. EXPERIMENTAL DETAILS

Full details of the growth of three InP:C epitaxial layers with increasing carbon contents, derived primarily from CCl_4 , have been presented in Ref. 6. We shall be concerned here with the two wafers labeled MR949 (the most highly doped layer) and MR950 (the second most highly doped layer), with total carbon contents of 1.0×10^{19} and $4.2 \times 10^{18} \text{ cm}^{-3}$, respectively, as determined by SIMS. Pairs of samples were cut from adjacent locations of each wafer and were subjected to rapid transient anneals (RTA) for 5 min at 500 °C, 600 °C, 700 °C or 800 °C in flowing argon. Heat treatment of samples in face-to-face contact led to the complete destruction of the epitaxial layers. This problem was overcome by coating the layers with SiO_2 to a thickness of 1.2 μm . The SiO_2 was deposited by plasma-enhanced chemical vapor deposition using a mixture of 5% silane (SiH_4) in N_2 and N_2O gases (1 Torr: 13.56 MHz; 24 W: 300 °C), similar to that described in Ref. 18. After a RTA, the SiO_2 layer was removed by dipping the sample in hydrofluoric acid.

Room-temperature Hall-effect measurements using the van der Pauw geometry with indium dot contacts made at a temperature below 350 °C showed that the MR949 and MR950 samples remained semi-insulating up to, and including, 700 °C. An exception was a sample of MR950, annealed at 600 °C, that became slightly *p*-type with $p = 6 \times 10^{15} \text{ cm}^{-3}$. After anneals at 800 °C, the samples showed weak *n*-type conductivity with $n \sim 10^{16} \text{ cm}^{-3}$. Epilayer thicknesses of 8.0 μm (MR949) and 10.3 μm (MR950) had been determined previously from SIMS measurements but varied by $\pm 5\%$ across the 2-in. wafer.⁶

IR-absorption measurements of each sample were made at $\sim 10 \text{ K}$ using a Bruker IFS 120 HR interferometer with a spectral resolution of 0.02 cm^{-1} and compared with corresponding data for the as-grown wafers (Table I). Calibration factors, $f(C_p)$ and $f(H-C_p)$, are required to determine impurity concentrations from values of the integrated absorption coefficients (IA) of the C_p and the $H-C_p$ LVM's, respectively: the concentrations are given by $f(\text{cm}^{-1}) \times \text{IA}(\text{cm}^{-2})$. Since these calibration factors have not been determined for InP the concentrations were estimated using the factors for the corresponding centers in GaAs (see the caption of Table I and Ref. 6).

Low-temperature (77 K) Raman measurements were made in the back-scattering geometry from the (100) growth surface using excitation from a Kr^+ -ion laser with $h\nu_L = 3.00$ or 3.05 eV. The scattered light, recorded for the $x(z,z)$ - x or $x(y,z)$ - x scattering configurations, where x , y , and z denote $\langle 100 \rangle$ crystallographic directions, was dispersed in a triple spectrometer and detected with a silicon charge-coupled detector (CCD) array. Measurements were made for the spectral ranges from 60 – 2200 and 3000 – 4500 cm^{-1} for samples of MR949, as described above. The Raman probe depth, $1/(2\alpha) \cong 17$ nm, where α is the absorption coefficient, was derived for photons with an energy of 3.00 eV using the data for the room-temperature dielectric function given in Ref. 19 and the temperature dependence of the band gap given in Ref. 20. Further Raman measurements were made after samples had been chemically etched to remove a surface layer of thickness of ~ 1 μm to determine whether this region, that had been in contact with the layer of SiO_2 , was representative of the bulk.

III. RESULTS

A. IR measurements of the modes of isolated carbon atoms and H-C_p pairs

After an anneal at 500°C , the same as the growth temperature, IR measurements showed *increases* in $[C_p]$ of $8 \times 10^{17} \text{cm}^{-3}$ for both samples MR949:(500°C) and MR950:(500°C) and *decreases* in $[H-C_p]$ of 8×10^{17} and $1 \times 10^{17} \text{cm}^{-3}$, respectively, that are attributed to dissociation of the pairs (Table I). The net gain of carbon in sample MR950:(500°C) implies that other sources of carbon must have been present and since the annealed samples remained semi-insulating, there must have been increases in the concentration of compensating donor centers (see Sec. III C). Anneals of both sets of samples at higher temperatures of 600 , 700 , and 800°C led to progressive *reductions* in $[C_p]$ (Figs. 1 and 2), implying the formation of carbon aggregates that are not IR active.

There were also reductions in the strengths of the three modes that are attributed to H-C_p pairs in MR949: these are the A_1^- -antisymmetric stretch mode at 2703.3cm^{-1} , the A_1^+ -symmetric stretch mode at 413.5cm^{-1} , and a transverse E mode at 521.1cm^{-1} with dominant carbon displacements: the E mode with dominant hydrogen displacements is not detected, consistent with its expected low dipole moment, as found for the corresponding mode of H-C_{As} pairs in GaAs.⁸ Measurements of the three H-C_p lines following anneals at temperatures up to 700°C demonstrate that their strengths are correlated (Fig. 3): the H-C_p pair lines are not detected after the 800°C anneal. Satellite lines at 2756cm^{-1} ($\Delta \sim 10 \text{cm}^{-1}$) and 2818cm^{-1} ($\Delta = 6 \text{cm}^{-1}$) on the high-energy side of the H-C_p A_1^- -stretch mode (MR949) had strengths of only $\sim 3\%$ of that of the main line and are similar to satellite lines detected in highly doped GaAs:C due to paired substitutional carbon atoms complexed with a hydrogen atom.^{21,22} After the anneal at 600°C , absorption from these lines in InP was below the detection limit. It is inferred that there is dissociation of the centers, with subsequent out-diffusion of the hydrogen or the formation of internal hydrogen clusters.

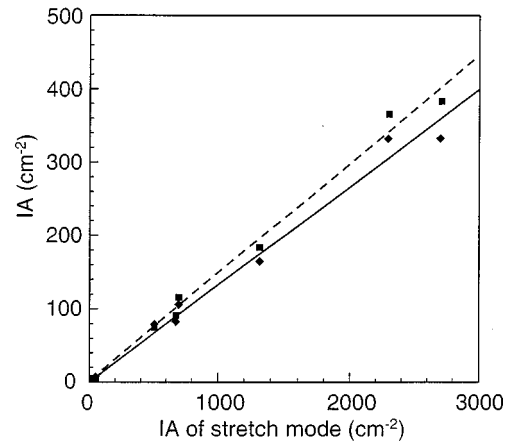


FIG. 3. Plot showing the correlations of the integrated absorptions (IA's) of the IR LVM at 521cm^{-1} (squares, E mode) and the IR LVM at 414cm^{-1} (diamonds, A_1^+ mode) as a function of the IA of the IR LVM at 2703cm^{-1} (A_1^- stretch mode) for samples MR950 and MR949 before and after annealing. The dashed (solid) line is a least-square fit to the squares (diamonds) and has a gradient of 0.150 (0.134).

Following anneals at 600°C and 700°C the MR949 and MR950 samples were still semi-insulating but after the final anneal at 800°C , they showed weak n -type conductivity with $n = 3.0 \times 10^{14}$ and $1.7 \times 10^{16} \text{cm}^{-3}$, respectively. These concentrations are negligible compared with the residual values of $[C_p] \sim 1.5 \times 10^{18} \text{cm}^{-3}$ that would give rise to strong p -type conductivity unless compensating donor centers or hole traps were still present.

B. Analysis of the line shape of the isolated carbon vibrational mode

The theoretical profiles that result from random electric-field broadening are given by a normalized universal function, $G(\omega/\omega^*)$, where ω^* is a scaling frequency.^{7,17} The function is generated from splittings of the InP:C triplet LVM absorption line produced from the statistically distributed electric fields at the C_p atom that arise from all possible configurations of surrounding charged impurities. In addition to the distribution of field strengths that follows a function due originally to Holtsmark,²³ the random distribution of field orientations is required. The scaling frequency ω^* is proportional to the $2/3$ power of the concentration of the surrounding charged impurities. This follows from the field strengths from point charges falling off as the inverse square of their distance from the center. Provided that the charge compensation mechanism is the same for all the samples, the concentration of the surrounding charged impurities will be proportional to the IA for the carbon acceptors.

To account for other sources of broadening, such as inhomogeneous strain from point defects or dislocations, limited instrumental resolution, and three-phonon decay, each of the sharp lines formed by splitting the triplet with a particular electric field is replaced by a profile characterized by γ , its half-width at half maximum (i.e., $\Delta/2$). The form of the profile will depend on the relative strengths of these sources:

TABLE II. Details of electric-field broadening for sample MR949. h_{expt} is the experimental peak height above a baseline taken between 543 and 551 cm^{-1} . The values of the integrated absorption (IA), measured from the same base line, are smaller by up to $\sim 10\%$ than those that can be inferred from the concentrations listed in Table I due to a different choice of base line.

	IA (cm^{-2})	h_{expt} (cm^{-1})	ω^* (cm^{-1})	$\frac{\omega^*}{(\text{IA})^{2/3}}$	γ (cm^{-1})
As grown	748	670	0.24	0.002 91	0.07
500 °C anneal	899	694	0.27	0.002 90	0.08
600 °C anneal	718	675	0.24	0.002 99	0.06
700 °C anneal	337	436	0.18	0.003 72	0.04
800 °C anneal	172	297	0.12	0.003 88	0.04

see, for example, Ref. 24 where theoretical analyses indicate that dislocations give rise to nearly Gaussian profiles, whereas point defects lead to Lorentzian profiles. As in our earlier work,^{7,17} we assume a Lorentzian form. The normalized theoretical profile for the broadened triplet is completely specified by the two parameters ω^* , the scaling frequency, and γ , the residual half-width.

From Fig. 4 of Ref. 17 it is clear that the overall width of the theoretical profile does not depend appreciably on the value used for γ provided that it is small compared with ω^* . For $\gamma=0$, the central feature is logarithmically divergent and the profile displays prominent shoulders. As γ is increased, the peak height is reduced and the shoulders become less pronounced. We may therefore choose ω^* by fitting to the overall width of an experimental profile and, after scaling the (normalized) theoretical profile to achieve agreement with the observed IA, adjusting γ to give the experimental peak height. Values for experimental IA's and peak heights are given in Tables II and III. Reasonably good representations of the shoulders result without any further adjustment to the parameters. As an illustration of the fitting procedure, we show in Fig. 4 a section of the experimental profile, including the shoulders and the peak, for sample MR949 annealed at 600 °C compared with three choices of ω^* taking, in each case, a value of γ that reproduces the peak height. With $\omega^*=0.24 \text{ cm}^{-1}$ there is good agreement with experiment on the low-frequency side of the absorption peak but less good agreement on the high-frequency side. The theoretical profile is symmetric about the peak and cannot reproduce the asym-

TABLE III. Details of electric-field broadening for sample MR950. h_{expt} is the peak height above a base line taken 544 and 550 cm^{-1} . Comments on IA are the same as in Table II.

	IA (cm^{-2})	h_{expt} (cm^{-1})	ω^* (cm^{-1})	$\frac{\omega^*}{(\text{IA})^{2/3}}$	γ (cm^{-1})
As grown	339	435	0.15	0.003 09	0.060
500 °C anneal	451	584	0.18	0.003 06	0.041
600 °C anneal	349	519	0.15	0.003 08	0.039
700 °C anneal	404	572	0.18	0.003 29	0.032
800 °C anneal	254	436	0.15	0.003 74	0.025

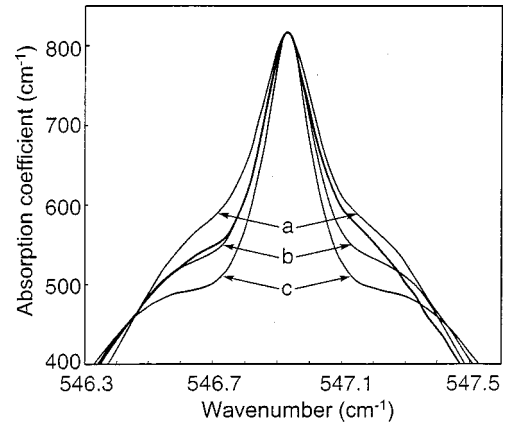


FIG. 4. Example of the fitting procedure applied to the profile of the C_P LVM for sample MR949 annealed at 600 °C with only the central peak and the shoulders displayed. The scale of the absorption coefficients is offset to coincide with the experimental data shown in Fig. 1. Theoretical profiles are shown as the thinner lines (*a, b, c*) for three choices of the scaling frequency ω^* : in order from the highest to the lowest shoulders, $\omega^*=0.21, 0.24,$ and 0.27 cm^{-1} . In each case, the residual half-width is determined by forcing agreement with the peak value for the experimental profile (shown as the thicker line): (a) $\gamma=0.078 \text{ cm}^{-1}$, (b) 0.061 cm^{-1} , and (c) 0.048 cm^{-1} , respectively. (The scale for the absorption coefficients is offset to agree with the display in Fig. 1.)

metry of the experimental spectra. Fitted compromise values for ω^* and γ are listed in Tables II and III.

From the results in Tables II and III, proportionality between ω^* and IA to the 2/3 power appears to be remarkably well satisfied for the two samples in their as-grown state and after the 500 °C and 600 °C anneals. Another roughly equal proportionality constant emerges for samples MR949:(700 °C), MR949:(800 °C), and MR950:(800 °C) [but not for MR950:(700 °C)]. It is possible that another compensation mechanism comes into play for samples annealed at 700 °C or above. The increase in $\omega^*/(\text{IA})^{2/3}$ for the high-temperature anneals would be explained if the reductions in $[C_P]$ are smaller than the reductions of the concentrations of other charged defects that are present.

The fitted residual half-width γ decreases from 0.06 to 0.025 cm^{-1} as the anneal temperature is increased for MR950 (Table III). The slightly larger values found for the MR949 sample (Table II) are consistent with the higher strain and a small shift in the lattice parameter revealed by high-resolution x-ray data⁶ for the as-grown wafer. All the values of γ are significantly greater than the instrumental IR resolution of 0.02 cm^{-1} , demonstrating that the broadening is not limited for this reason. It is implied that there must have been modifications of the compensation process and/or reductions of inhomogeneous strains as a result of the annealing.

C. Raman scattering measurements

Raman measurements made on an as-grown sample of MR949 reveal the LVM of $^{12}\text{C}_P$ at 546.5 cm^{-1} (Fig. 5), as found by IR absorption.⁶ The scattering strength with an in-

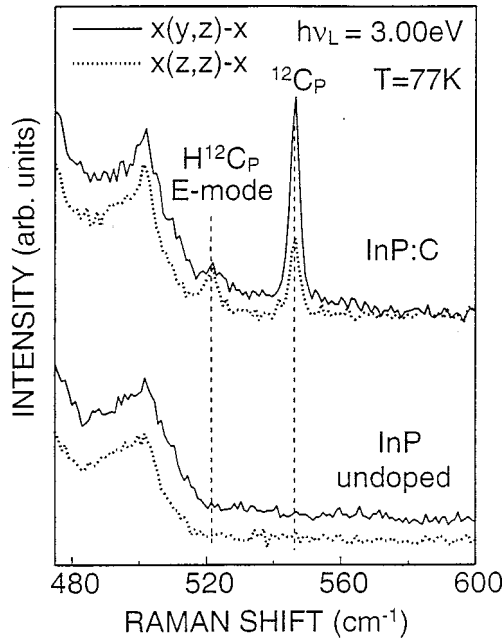


FIG. 5. Low-temperature (77 K) Raman spectra recorded in the $x(x,z)-x$ and $x(z,z)-x$ scattering configurations from the as-grown InP:C sample MR949 and a reference spectrum from undoped InP. The spectra show the $^{12}\text{C}_P$ LVM and an E mode of the $\text{H-}^{12}\text{C}_P$ complex. The spectral resolution was set to 2.5 cm^{-1} .

cident laser energy of 3.00 eV is stronger by a factor of ~ 2.5 for the $x(y,z)-x$ geometry than that for the $x(z,z)-x$ geometry. The nonzero scattering for the $x(z,z)-x$ geometry is explained by roughening of the surface of the sample during growth of the epilayer: greater roughening is expected following the etching of samples, see below. This scattering at 546.5 cm^{-1} is attributed to an $F_2(T_2)$ mode of a $^{12}\text{C}_P$ center with T_d symmetry.²⁵

As expected from the IR data, the scattering intensity at 77 K of the C_P line in the as-grown MR949 sample was stronger by a factor of ~ 2.7 than that from the MR950 sample using a laser energy of 3.00 eV (Fig. 6) or 3.05 eV: the strength of the intrinsic InP second-order phonon scattering was used as an internal reference. As the strength of the line in MR950 was only ~ 3 times greater than the noise level, it was too small to be investigated by Raman scattering following anneals of the samples. The intensity at 77 K of the C_P line for unetched MR949 samples after anneals at 500°C , 600°C , and 700°C showed only small changes (Fig. 7) but a later second set of measurements revealed a reduction in $[\text{C}_P]$ by $\sim 40\%$ after the 700°C anneal. This difference is attributed to nonuniformity of the surface roughness. The line was not detected in the sample annealed at 800°C ($< 8\%$ of the as-grown sample). These measurements are in essential agreement with the IR data (Table I).

The observed polarization dependence of the 521-cm^{-1} Raman line (cf. IR frequency of 521.1 cm^{-1}) due to H-C_P pairs is compatible with the assignment to a transverse E mode, although the strength of this argument is limited by the poor signal-to-noise ratio (Fig. 5). The lack of observation of an E mode with dominant hydrogen displacements was not surprising as the corresponding mode of H-C pairs

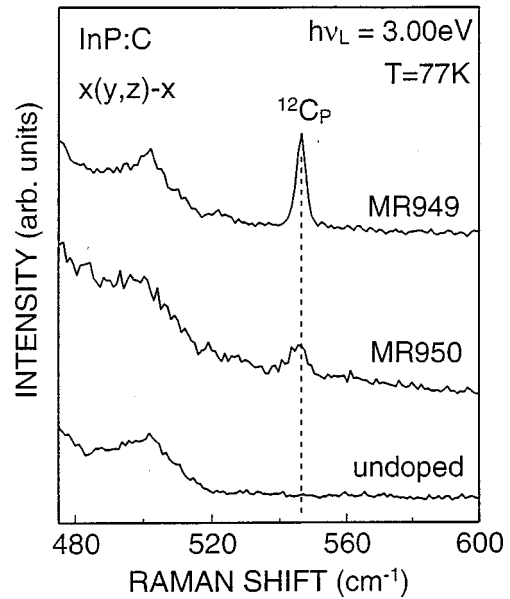


FIG. 6. Comparison of the Raman scattering strengths of the $^{12}\text{C}_P$ LVM in InP:C with different carbon contents for the as-grown samples MR949 and MR950. For comparison, the Raman spectrum of undoped InP is also displayed. The spectral resolution was set to 2.5 cm^{-1} .

in GaAs is extremely weak.²⁶ The absence of a line due to the A_1^+ mode is explained by the use of laser excitation energies of 3.00 or 3.05 eV that are smaller than the InP $E_1/(E_1 + \Delta)$ band gap of $3.25\text{--}3.38\text{ eV}$ at 77 K (see Sec. II), precluding resonant enhancements as found for the A_1^+ mode of H-C_P pairs in GaAs.²⁷ Corresponding enhancement effects

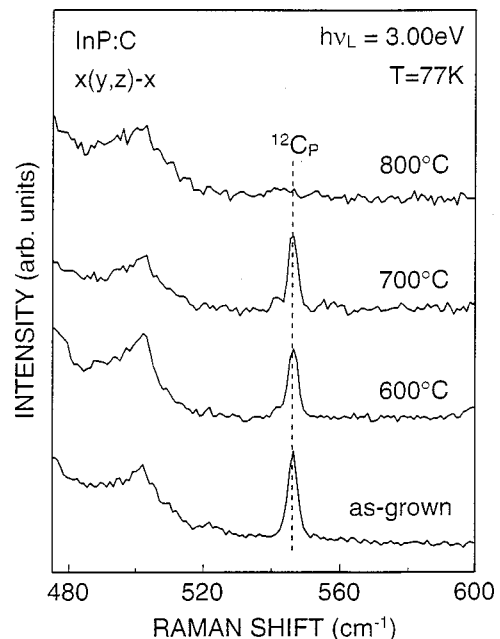


FIG. 7. The dependence of the Raman scattering strength of the $^{12}\text{C}_P$ LVM as a function of the anneal temperature for samples of wafer MR949. The spectral resolution was 2.5 cm^{-1} .

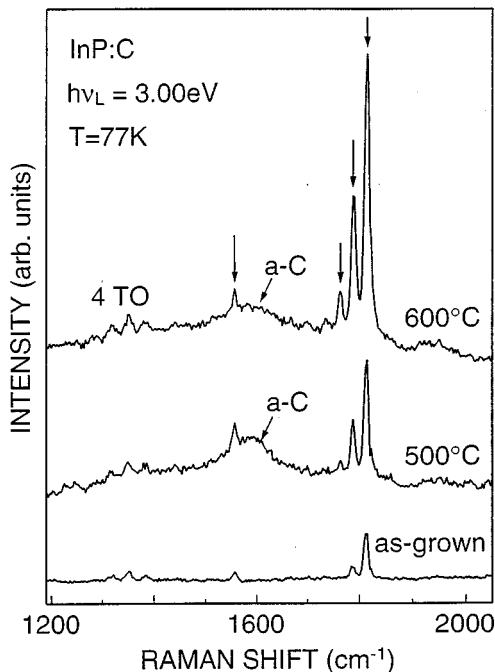


FIG. 8. Spectra of high-frequency Raman lines from as-grown and annealed InP:C samples from wafer MR949. Raman lines due to carbon complexes in InP:C are marked by vertical arrows; *a*-C denotes Raman scattering from amorphous carbon. Spectral resolution was 7 cm^{-1} .

for InAs and InSb are reported in Ref. 28. Finally, the absence of detectable scattering from the A_1^- stretch mode is not inconsistent with the small signal-to-noise ratio found for this mode in GaAs (Ref. 27) and AlAs.²⁹

The surfaces of an as-grown sample, and samples annealed at 500°C and 600°C , were extremely rough following etching to a depth of $\sim 1 \mu\text{m}$ (see Sec. II), as indicated by intense elastic scattering from the gas discharge lines of the Kr^+ laser, and the C_p lines were not resolved. An etched sample annealed at 700°C did, however, show the C_p line but with a strength of only 15% of that for the unetched, as-grown sample. The C_p line was not observed in the etched sample annealed at 800°C . It could be inferred that the value of $[C_p]$ in the bulk of the 700°C annealed material is somewhat lower than that in the region close to the as-grown interface with the original surface SiO_2 layer. However, the difference is more likely to be due to the wet chemical-etching process adding to the surface roughness already present as a result of the prior plasma processing³⁰ and the removal of the SiO_2 layer by HF acid.

Of greatest importance are the observations of Raman scattering at 1784.9 and 1814 cm^{-1} from the as-grown MR949 sample (Fig. 8). The strengths of these modes *increased* in the same ratio following anneals at 500°C and 600°C and a correlated third line appeared and grew at 1763.7 cm^{-1} . There were no further changes after the 700°C anneal but after the 800°C anneal, the lines were no longer resolved due to strong background scattering and/or luminescence that occurred in the range 1000 – 2000 cm^{-1} . Essentially identical results were obtained for the etched samples.

An additional line at 1557.9 cm^{-1} , together with a broad vibrational band ($\Delta \sim 70 \text{ cm}^{-1}$) centered around 1580 cm^{-1} , not present in the spectra of as-grown samples, appeared after the anneals at 600°C and the band became very strong after the 700°C anneal. The broadband is characteristic of amorphous carbon^{12,31,32} and appeared with similar strengths in both the unetched and etched samples. These observations demonstrate that carbon precipitates formed in the bulk of the samples during annealing and were not present only as surface contamination. The first stage of aggregation is clearly C-C formation.

H_2 molecules may have formed by the pairing of hydrogen atoms released from H- C_p pairs during the anneals but an associated vibrational frequency at $\sim 4000 \text{ cm}^{-1}$ was not detected. This does not necessarily imply that molecules were absent as they have only been reported at concentrations in the range 10^{19} – 10^{20} cm^{-3} in GaAs samples following exposure to a hydrogen plasma.³³

IV. DISCUSSION

Assignments of the Raman LVM lines in the range 1763 – 1814 cm^{-1} to dicarbon centers are inferred from comparisons with corresponding lines observed in GaAs:C and AlAs:C.^{12,13} The loss during anneals of $^{12}\text{C}_{\text{As}}$ and $^{13}\text{C}_{\text{As}}$ acceptors, present in nearly equal concentrations in doped GaAs, led to the formation of two types of split-interstitial dicarbon C-C centers (non-IR-active O_2 molecules) that were each unambiguously identified by Raman scattering as ^{12}C - ^{12}C , ^{12}C - ^{13}C , and ^{13}C - ^{13}C pairs. *Ab initio* calculations¹³ demonstrated that the C-C defects were located on As lattice sites in the positive charge state and that the molecules could be present in either of two inequivalent orientations. Corresponding centers (labeled T1 and T2) were also observed in AlAs. The pairs of ^{12}C - ^{12}C modes in the two lattices have the same mean frequency of $\sim 1800 \text{ cm}^{-1}$ but with line separations of 87 and 96 cm^{-1} , respectively. The two strong lines at 1784.9 and 1814.0 cm^{-1} , observed in the present InP:C samples, also have a mean energy of $\sim 1800 \text{ cm}^{-1}$ but with a smaller separation of 25 cm^{-1} and relative strengths in the opposite sense to those in GaAs and AlAs. Whereas the as-grown GaAs and AlAs samples were very strongly *p* type, and remained *p* type after annealing, the InP samples were fully compensated. The two C-C centers in the former materials were therefore identified as ionized deep donor defects in the positive charge state. The related defects in the present InP samples might be negatively charged, neutral, or positively charged during examination, since account must be taken of photoexcitation due to the incident laser radiation required to make the Raman measurements. Changes in the charge states of the C-C centers leads to shifts in the LVM frequencies according to the *ab initio* calculations for GaAs and AlAs.¹³ In the absence of illumination, C-C donors would compensate some fraction of the isolated carbon acceptors in the as-grown InP layers and the remaining C_p acceptors would be passivated by hydrogen atoms. It has been demonstrated that $[C-C]$ increases as the anneal temperature is raised and at some stage may exceed the remaining $[C_p]$. Since the excess dicarbon centers are deep defects,

any increase in the carrier concentration at room temperature is expected to be small but could account for the measured n -type conductivity of the samples that had been annealed at 800 °C.

Dicarbon centers can only form if carbon atoms make diffusion jumps to interstitial sites and then diffuse and are trapped by remaining substitutional carbon atoms. A discussion of this process for GaAs and AlAs is given in Ref. 34 and the diffusion activation energy is calculated to be 0.7 eV for both host crystals. As the anneal temperature is increased the diffusion coefficient of the interstitial carbon atoms would increase, consistent with the increased formation of amorphous carbon inclusions. There is evidence that the bonding of carbon atoms to In neighbors is weaker than that to Ga or Al neighbors.³⁵ As a consequence, the transfer of carbon atoms to interstitial sites in InP is likely to occur more readily than in GaAs or AlAs, allowing rapid formation of the observed C-C centers. The formation of C-C centers could reduce the strain in the InP and lead to reductions in γ (Sec. II B).

The possibility that other donor centers ($V_{\text{In}}\text{H}_4$, C_{In} , and P_{In}) were present was also considered. The IR LVM (Ref. 9) of $V_{\text{In}}\text{H}_4$ donors at 2316 cm^{-1} was observed in our as-grown InP substrates that were wedged and had thicknesses of ~ 300 μm . The measured integrated absorption coefficient (IA) of $0.10 \pm 0.02 \text{ cm}^{-2}$ leads to $[V_{\text{In}}\text{H}_4] = 4.5 \times 10^{15} \text{ cm}^{-3}$ using the calibration that an IA of 1 cm^{-2} corresponds to a concentration of $4.5 \times 10^{16} \text{ cm}^{-3}$.³⁶ The combined IA's of the substrate and the epitaxial layers were no greater than the values for the substrate alone, implying that the concentration of $V_{\text{In}}\text{H}_4$ complexes incorporated in the layers must have been less than $\sim 4.5 \times 10^{16} \text{ cm}^{-3}$. The measured IA decreased after the sample had been annealed at 700 °C and was not detected after the anneal at 800 °C, consistent with other reports.^{11,36} Thus, $[V_{\text{In}}\text{H}_4]$ is smaller by a factor of $\sim 10^2$ than that required to compensate the carbon acceptors in the epitaxial layers.

We considered the possibility that C_{In} donors, as well as carbon acceptors C_{P} , were introduced into the samples during growth. According to *ab initio* local-density-functional calculations, the frequency of the donor LVM is lower than that of the acceptor by 30 cm^{-1} .³⁷ This would place the C_{In} LVM frequency at 517 cm^{-1} , which is at the steep edge of the spectral region where there is strong two-phonon absorption. A line has not been detected and so there is no evidence that these centers were present. The possibility that the gap mode (GM) at 220 cm^{-1} reported in Ref. 5 is due to C_{In} donors cannot be ruled out since the epitaxial layers were grown under quite different conditions from those studied here but the expected LVM in these samples was not detected.

The intrinsic antisite double donor defect $^{31}\text{P}_{\text{In}}$ is expected to give rise to both an LVM and a GM (see Ref. 38), both of which should be IR and Raman active. The LVM is expected to have a lower frequency than that of $^{30}\text{Si}_{\text{In}}$ single donors³⁹

based on the sequence ($^{28}\text{Si}_{\text{In}}$ 92.3% at 431.6 cm^{-1}), ($^{29}\text{Si}_{\text{In}}$ 4.7% at 427.1 cm^{-1}), and ($^{30}\text{Si}_{\text{In}}$ 3.0% at 423.1 cm^{-1}) with the assumption that the local force constants are similar. No such LVM has been observed. A weak gap mode at 209.86 cm^{-1} ($\Delta = 0.16 \text{ cm}^{-1}$) observed in two Si-doped bulk samples is tentatively attributed to $^{28}\text{Si}_{\text{In}}$; no corresponding GM from $^{31}\text{P}_{\text{In}}$ at a somewhat lower energy was found in either the bulk or the epitaxial InP. Two GM's observed at 281.1 and 284.6 cm^{-1} in the epilayers are of unknown origin. Likewise, a cluster of seven lines with frequencies between 351 and 360 cm^{-1} and linewidths $\Delta \sim 0.3 \text{ cm}^{-1}$, detected from the as-grown samples MR949 and MR950, are also of unknown origin. The two GM's and these lines started to anneal at 600 °C and were not detected after the 700 °C heat treatment. We cannot rule out the possibility that these various lines may be related to $^{31}\text{P}_{\text{In}}$ antisite defects as three types of defects have been observed by optically detected electron nuclear double resonance⁴⁰ (ODENDOR) and it has been reported that they are stable up to 500 °C.⁴¹ On the other hand, there is no clear evidence for the presence of P_{In} defects.

V. SUMMARY AND CONCLUSIONS

In summary, the compensation of the carbon acceptors in the as-grown epitaxial layers is explained by the presence of H-C pairs and deep dicarbon donor centers without invoking the presence of other types of donor. Subsequent heat treatments lead to the dissociation of the H-C defects and there are losses of carbon acceptors from solution. During these anneals carbon atoms must jump into interstitial sites and diffuse to form dicarbon defects, and larger amorphous carbon precipitates,³² both of which are only revealed by Raman scattering. No evidence has been found for the incorporation of $V_{\text{In}}\text{H}_4$, C_{In} , or P_{In} donors in these samples and it is considered unlikely that these centers play a role in the compensation process. After the higher-temperature anneals, the continuing presence of dicarbon centers maintains the compensation up to 700 °C. The formation of dicarbon centers and amorphous carbon with the concomitant loss of carbon acceptors continues at 800 °C and is expected to lead to excess deep donors so that the samples would become slightly n -type at room temperature, as found experimentally. This excess of donors, together with the reduction in $[C_{\text{P}}]$ will reduce the number of strain centers and it is likely that the dicarbon defect will strain the lattice less than the small carbon atoms. This may explain the sharpening of the C_{P} LVM profile (Tables II and III).

ACKNOWLEDGMENTS

The authors thank J. C. Clark and G. Hill (Sheffield University) for coating the samples with SiO_2 . B.R.D. and R.C.N. thank the Engineering and Physical Sciences Research Council, UK, for their financial support (Grant No. GR/K 96977).

- * Author to whom all correspondence should be addressed: Email address: m.j.l.sangster@reading.ac.uk
- ¹N. F. Gardner, Q. H. Hartmann, S. A. Stockman, G. E. Stillman, J. E. Baker, J. I. Malin, and K. C. Hsieh, *Appl. Phys. Lett.* **65**, 359 (1994).
 - ²N. F. Gardner, Q. H. Hartmann, J. E. Baker, and G. E. Stillman, *Appl. Phys. Lett.* **67**, 3004 (1995).
 - ³C. R. Abernathy, in *State of the Art Program on Compound Semiconductors, XXIV*, edited by F. Ren, S. J. Pearton, S. N. G. Chu, R. J. Shul, W. Pletchen, and T. Kamijo (The Electrochemical Society, Pennington, NJ, 1996), Vol. 96-2, pp. 1–18 and references therein.
 - ⁴J-H. Oh, J. Shirakashi, F. Fukuchi, and M. Konagai, *Appl. Phys. Lett.* **66**, 2891 (1995).
 - ⁵M. Ramsteiner, P. Kleinert, K. H. Ploog, J-H. Oh, M. Konagai, and Y. Takahashi, *Appl. Phys. Lett.* **67**, 647 (1995).
 - ⁶B. R. Davidson, R. C. Newman, and C. C. Button, *Phys. Rev. B* **58**, 15 609 (1998).
 - ⁷R. C. Newman, B. R. Davidson, R. S. Leigh, M. J. L. Sangster, and C. C. Button, *Physica B* **273-274**, 827 (1999).
 - ⁸B. R. Davidson, R. C. Newman, T. J. Bullough, and T. B. Joyce, *Phys. Rev. B* **48**, 17 106 (1993).
 - ⁹R. Darwich, B. Pajot, B. Rose, D. Bobein, B. Theys, R. Rhabi, C. Porte, and F. Gendron, *Phys. Rev. B* **48**, 17 776 (1993).
 - ¹⁰F. X. Zach, E. E. Haller, D. Gabbe, G. Iseler, G. G. Bryant, and D. F. Bliss, *J. Electron. Mater.* **25**, 331 (1996).
 - ¹¹W. M. Chen, P. Dreszer, A. Presad, W. Kurpiewski, W. Walukiewicz, E. R. Weber, E. Söman, B. Monemar, B. W. Liang, and C. W. Tu, *J. Appl. Phys.* **76**, 600 (1994).
 - ¹²J. Wagner, R. C. Newman, B. R. Davidson, S. P. Westwater, T. J. Bullough, T. B. Joyce, C. D. Latham, R. Jones, and S. Öberg, *Phys. Rev. Lett.* **78**, 74 (1997).
 - ¹³B. R. Davidson, R. C. Newman, C. D. Latham, R. Jones, J. Wagner, C. C. Button, and P. R. Briddon, *Phys. Rev. B* **60**, 5447 (1999).
 - ¹⁴Byoung-Ho Cheong and K. J. Chang, *Phys. Rev. B* **49**, 17 436 (1994).
 - ¹⁵B. Ulrici and E. Jahne, *Phys. Status Solidi B* **74**, 601 (1976).
 - ¹⁶R. C. Newman, F. Thompson, J. B. Mullin, and B. W. Straughan, *Phys. Lett.* **33A**, 113 (1970).
 - ¹⁷R. S. Leigh, M. J. L. Sangster, and R. C. Newman, *Phys. Rev. B* **60**, 10 845 (1999).
 - ¹⁸B. S. Sahu, O. P. Aginhoti, S. C. Jain, R. Mertens, and I. Kato, *Semicond. Sci. Technol.* **15**, L11 (2000).
 - ¹⁹D. E. Aspnes and A. A. Studna, *Phys. Rev. B* **27**, 985 (1983).
 - ²⁰P. Lautenschlager, M. Garriga, and M. Cardona, *Phys. Rev. B* **36**, 4813 (1987).
 - ²¹D. M. Kozuch, M. Stavola, S. J. Pearton, C. R. Abernathy, and W. S. Hobson, *J. Appl. Phys.* **73**, 3716 (1993).
 - ²²B. R. Davidson, R. C. Newman, H. Fushimi, K. Wada, and N. Inoue, *J. Appl. Phys.* **81**, 7255 (1997).
 - ²³J. Holtzmark, *Ann. Phys. (Leipzig)* **58**, 577 (1919).
 - ²⁴A. M. Stoneham, *Rev. Mod. Phys.* **41**, 82 (1969).
 - ²⁵D. T. Hon, W. L. Faust, W. G. Spitzer, and P. F. Williams, *Phys. Rev. Lett.* **25**, 1184 (1970).
 - ²⁶J. Wagner, K. H. Bachem, B. R. Davidson, R. C. Newman, T. J. Bullough, and T. B. Joyce, *Phys. Rev. B* **51**, 4150 (1995).
 - ²⁷J. Wagner, M. Maier, Th. Lauterback, K. H. Bachem, M. J. Ashwin, R. C. Newman, K. Woodhouse, R. Nicklin, and R. R. Bradley, *Appl. Phys. Lett.* **60**, 2546 (1992).
 - ²⁸J. Wagner, P. Koidl, and R. C. Newman, *Appl. Phys. Lett.* **59**, 1729 (1991).
 - ²⁹J. Wagner, R. E. Pritchard, B. R. Davidson, R. C. Newman, T. J. Bullough, T. B. Joyce, C. Button, and J. S. Roberts, *Semicond. Sci. Technol.* **10**, 639 (1995).
 - ³⁰J. R. Botha, J. H. Neethling, and A. W. R. Leitch, *Semicond. Sci. Technol.* **14**, 1147 (1999).
 - ³¹A. J. Moll, E. E. Haller, J. W. Ager III, and W. Walukiewicz, *Appl. Phys. Lett.* **65**, 1145 (1994).
 - ³²A. J. Moll, J. W. Ager III, Kim Man Yu, W. Walukiewicz, and E. E. Haller, *Inst. Phys. Conf. Ser.* **141**, 269 (1995).
 - ³³J. Vetterhöffer, J. Wagner, and J. Weber, *Phys. Rev. Lett.* **77**, 5409 (1996).
 - ³⁴C. D. Latham, R. Jones, M. Haugk, Th. Frauenheim, and P. R. Briddon, *Physica B* **273-274**, 784 (1999).
 - ³⁵R. E. Pritchard, R. C. Newman, J. Wagner, M. Maier, A. Mazuelas, K. H. Ploog, P. A. Lane, T. Martin, and C. R. Whitehouse, *Appl. Phys. Lett.* **66**, 2676 (1995).
 - ³⁶J. A. Wolk, G. Iseler, G. G. Bryant, E. D. Bourret-Courchesne, and D. F. Bliss, *Proceedings of the International Conference on InP and Related Materials*, Cape Cod, MA, 1997 (IEEE, New York, 1997), p. 408.
 - ³⁷C. D. Latham (private communication).
 - ³⁸R. C. Newman, *Infrared Studies of Crystal Defects* (Taylor & Francis, London, 1973).
 - ³⁹M. R. Brozel, R. C. Newman, and M. G. Astles, *J. Phys. C* **11**, L377 (1978).
 - ⁴⁰H. J. Sun, H. P. Gislason, C. F. Rong, and G. D. Watkins, *Phys. Rev. B* **48**, 17 092 (1993).
 - ⁴¹I. A. Buyanova, W. M. Chen, W. G. Bi, Y. P. Zeng, and C. W. Tu, *Appl. Phys. Lett.* **75**, 1733 (1999).